Monthly Notices
of the
ROYAL ASTRONOMICAL SOCIETY

Mon. Not. R. Astron. Soc. **410,** 775–787 (2011) doi:10.1111/j.1365-2966.2010.17480.x

The galaxies that reionized the Universe

Milan Raičević,[1,2★] Tom Theuns[1,3] and Cedric Lacey[1]

[1] *Institute for Computational Cosmology, Durham University, Science Laboratories, Durham DH1 3LE*
[2] *Leiden Observatory, Leiden University, PO Box 9513, 2300RA Leiden, the Netherlands*
[3] *Universiteit Antwerpen, Campus Groenenborger, Groenenborgerlaan 171, B-2020 Antwerpen, Belgium*

Accepted 2010 August 4. Received 2010 August 2; in original form 2010 July 9

ABSTRACT

The Durham GALFORM semi-analytical galaxy formation model has been shown to reproduce the observed rest-frame 1500-Å luminosity function of galaxies well over the whole redshift range $z = 5$–10. We show that in this model, this galaxy population also emits enough ionizing photons to reionize the Universe by redshift $z = 10$, assuming a modest escape fraction of 20 per cent. The bulk of the ionizing photons is produced in faint galaxies during starbursts triggered by galaxy mergers. The bursts introduce a dispersion up to ∼5 dex in galaxy-ionizing luminosity at a given halo mass. Almost 90 per cent of the ionizing photons emitted at $z = 10$ are from galaxies below the current observational detection limit at that redshift. Photoionization suppression of star formation in these galaxies is unlikely to affect this conclusion significantly, because the gas that fuels the starbursts has already cooled out of their host haloes. The galaxies that dominate the ionizing emissivity at $z = 10$ are faint, with $M_{1500,\mathrm{AB}} \sim -16$, have low star formation rates, $\dot{M}_\star \sim 0.06\,h^{-1}\,\mathrm{M}_\odot\,\mathrm{yr}^{-1}$, and reside in haloes of mass $M \sim 10^9\,h^{-1}\,\mathrm{M}_\odot$.

Key words: galaxies: evolution – galaxies: formation – galaxies: high-redshift – intergalactic medium – dark ages, reionization, first stars.

1 INTRODUCTION

Reionization refers to the transition in the state of the Universe from mostly neutral, following recombination at a redshift of $z \sim 1000$, to highly ionized once more at later times. Gunn & Peterson (1965) (and also Bahcall & Salpeter 1965) realized as soon as Schmidt (1965) published spectra of $z \sim 2$ quasars that the absence of significant Lyman α absorption in their spectra implied that the $z \sim 2$ Universe is very highly ionized. That basic picture has not changed with the discovery by Fan et al. (2003) of $z > 6$ QSOs (Becker, Rauch & Sargent 2007) or the novel method based on gamma-ray bursts as probes of the intergalactic medium (IGM) at even higher z (Totani et al. 2006; Patel et al. 2010; Zafar et al. 2010).

The fact that most of the hydrogen in the Universe is highly ionized at least as early as $z \sim 7$ is also consistent with the large Thomson scattering optical depth towards the surface of large scattering which is inferred from measurements of CMB fluctuations. This implies a 'reionization redshift' of $z_{\mathrm{reion}} = 10.5 \pm 1.2$, if the transition from neutral to completely ionized occurred instantaneously (Komatsu et al. 2010). The temperature of the IGM depends on its reionization history because the thermal time-scales are long: measurements of that temperature (Schaye et al. 2000) are also consistent with reionization occurring around $z \sim 10$ (Theuns et al. 2002).

The current paradigm as to how reionization happens is that initially small H II regions form around individual sources of ionizing photons.[1] As the sources become brighter and more numerous, isolated H II regions grow, merge and eventually percolate throughout the IGM; see for example the early simulations by Gnedin & Ostriker (1997). The nature of the sources of the ionizing radiation is still unknown. While a number of works show that the majority of ionizing radiation is probably produced by stellar sources (e.g. Madau, Haardt & Rees 1999; Gnedin 2000a; Ciardi, Stoehr & White 2003; Sokasian et al. 2003; Furlanetto, Zaldarriaga & Hernquist 2004; Trac & Cen 2007; Trac & Gnedin 2009), the exact contribution of Population III stars or quasars is under debate (see Choudhury & Ferrara 2007; Wyithe & Cen 2007; Loeb 2009; Volonteri & Gnedin 2009; Salvaterra, Ferrara & Dayal 2010, for recent examples).

Depending on its spin temperature, the not-yet ionized H I during the epoch of reionization (EoR) could be detected in either emission or absorption in redshifted 21-cm radiation, either in the form of a global step in the spectrum, or indeed probing the remaining neutral regions in a partly ionized IGM (Madau, Meiksin & Rees 1997; Shaver et al. 1999; Tozzi et al. 2000). Because most plausible ionizing sources will be highly clustered, the ionized bubbles could grow to be quite large, and the epoch where the IGM is

[1] However, a strong background flux of higher-energy radiation, for example X-rays from accreting black holes, may 'pre-reionize' the Universe (Oh 2001).

★E-mail: milan.raicevic@durham.ac.uk

50 per cent ionized may be best suited for direct detection with current and future experiments, such as LOFAR,[2] 21CMA,[3] MWA[4] and eventually the SKA.[5] The promise of a direct observational probe has stimulated considerable interest in the EoR; see recent reviews by for example Barkana & Loeb (2001); Ciardi & Ferrara (2005); Loeb (2006); Trac & Gnedin (2009).

The recent installation of the Wide Field Camera 3 (WFC3)/IR on the *Hubble Space Telescope* has made it possible to search for $z > 6$ galaxies using the 'Lyman-break' drop-out technique, with a number of authors reporting the discovery of galaxies with $z > 6$ (based on their colours), with candidates up to $z \sim 10$ (Bouwens et al. 2007; Bunker et al. 2009a; Bouwens et al. 2009, 2010; Oesch et al. 2009). Are these the galaxies that caused reionization? The analysis by Bunker et al. (2009b) suggests that these galaxies are unlikely to produce sufficient ionizing photons to reionize the Universe. In fact even at lower $z \sim 6$ there seems to be a problem, in the sense that the observed galaxies do not appear to produce sufficient photons to keep the IGM from recombining (Bolton & Haehnelt 2007).

In this paper we use the GALFORM semi-analytical model of galaxy formation (Cole et al. 2000; Baugh et al. 2005) to make theoretical predictions for the evolution of the emissivity of ionizing photons from galaxies, $\epsilon(z)$. The GALFORM model calculates the formation and evolution of galaxies in the framework of hierarchical structure formation in CDM, including baryonic physics such as gas cooling, star formation and supernova feedback. In contrast to most other work modelling the contribution of galaxies to reionization, the GALFORM model which we use here was originally developed to try to explain the properties of galaxies at much lower redshifts. Predictions from GALFORM have been compared with a very wide range of observational data at lower redshifts $z \lesssim 6$, including galaxy luminosity functions, colours, sizes, morphologies, gas contents and metallicities at redshift $z = 0$ (Cole et al. 2000; Baugh et al. 2005; Bower et al. 2006; González et al. 2009); the evolution of galaxies at optical, IR and sub-millimetre wavelengths (Baugh et al. 2005; Bower et al. 2006; Lacey et al. 2008; Gonzalez-Perez et al. 2009); and the evolution of Lyα-emitting galaxies (Le Delliou et al. 2006; Orsi et al. 2008). In this paper, we use the Baugh et al. (2005) variant of the GALFORM model. This model was already shown by Baugh et al. to reproduce the observed rest-frame far-UV luminosity function of Lyman-break galaxies at $z \sim 3$, and the same model has recently been shown to reproduce the observed numbers of Lyman-break galaxies over the whole range of $z \sim 3$–10 (Lacey et al. 2010a). Two important features of the Baugh et al. (2005) model are that at high redshifts, most star formation happens in starbursts triggered by galaxy mergers, and the initial mass function (IMF) of the stars formed in such bursts is top heavy, containing a much larger proportion of high-mass stars than is found in more quiescent star formation environments such as the solar neighbourhood. This top-heavy IMF was introduced into the model by Baugh et al. in order to explain the observed numbers and redshifts of the faint submillimetre galaxies, now known to be very luminous, dust-obscured starbursts at $z \sim 1$–3. Models assuming a standard solar neighbourhood IMF were found to underpredict the numbers of submillimetre galaxies by an order of magnitude, if these models were also constrained to reproduce the present-day galaxy luminosity functions.

In the present study, we want to investigate whether a model that is consistent with the new measurements of the Lyman-dropout galaxy population at $z > 6$ can produce sufficient ionizing photons to reionize the Universe at $z_{\rm reion} \gtrsim 10$. If so, we want to quantify which galaxies dominate ϵ, and which aspects of the model affect ϵ most. A similar analysis based on the GALFORM model was performed by Benson et al. (2006) (see also Benson et al. 2002a,b), who also included a simple model for the evolution of the H II volume filling factor. The present paper looks in more detail at the properties of the galaxies that cause reionization and the dark matter haloes that host them, and how these are connected to the newly discovered $z > 6$ drop-outs. The properties of Lyman-break galaxies predicted by GALFORM over the whole redshift range $z = 3$–20 have been analyzed in more detail in a companion paper by Lacey et al. (2010a), which also makes a more detailed comparison with the observed far-UV luminosity functions. We emphasize that the default values of the GALFORM model parameters used in the present work are identical to those chosen by Baugh et al. (2005), which were adjusted to match a range of observed galaxy properties at lower redshifts. We will couple the GALFORM source model with a radiative transfer scheme to investigate the progression of reionization in more detail in a follow-up paper (Raičević et al. 2010).

This paper is organized as follows. In Section 2 we briefly discuss the main ingredients of GALFORM, paying particular attention to those aspects that most affect the ionizing luminosities of the galaxies. In Section 3 we show the evolution of the emissivity ϵ for the default GALFORM parameters, discuss which galaxies dominate ϵ, and how changes in GALFORM parameters affect ϵ. In Section 4 we show the corresponding far-UV luminosity functions at $z = 6$ and 10, explore the extent to which the currently detected galaxies constrain ϵ, and how future observations with e.g. the *James Webb Telescope* will improve our understanding. We summarize in Section 5.

2 METHOD

The GALFORM semi-analytical model (Cole et al. 2000) computes how galaxies form and evolve in the hierarchically growing dark matter haloes of a cold dark matter Universe. The evolution of the haloes themselves is described by halo merger trees, which are either extracted from an *N*-body simulation or computed using a Monte Carlo scheme based on Lacey & Cole (1993) and improved by Parkinson, Cole & Helly (2008). The semi-analytical algorithm incorporates physically motivated recipes for gas cooling, star formation, feedback from supernovae, galaxy mergers, metal enrichment, dust production and other processes, and in particular allows a calculation of the observable properties of each galaxy, notably its broad-band luminosity and colours, and its ionizing emissivity; see Baugh (2006) for a recent review of semi-analytical methods.

The build-up of dark matter haloes of course depends on the assumed cosmological parameters, but the properties of the *galaxies* associated with them are at least equally strongly dependent on the 'gastrophysics' governed by GALFORM parameters; for this reason we only consider the cosmological parameters used in the Millennium simulation Springel et al. (2005), $(\Omega_{\rm m}, \Omega_\Lambda, \Omega_{\rm b}, h, \sigma_8, n_s) = (0.25, 0.75, 0.045, 0.73, 0.9, 1)$.[6]

[2] http://www.lofar.org/
[3] http://21cma.bao.ac.cn/
[4] http://www.haystack.mit.edu/ast/arrays/mwa/
[5] http://www.skatelescope.org/

[6] Note that the original Baugh et al. (2005) model used a slightly different cosmology, $(\Omega_{\rm m}, \Omega_\Lambda, \Omega_{\rm b}, h, \sigma_8, n_s) = (0.3, 0.7, 0.04, 0.7, 0.9, 1)$. The change of cosmological parameters was introduced for consistency with the Millennium-II simulation (Boylan-Kolchin et al. 2009) which we will employ in future numerical simulations of reionization.

Even at redshift $z = 0$ only a very small fraction of baryons have been converted into stars (Fukugita, Hogan & Peebles 1998). In particular the faint-end slope of the $z = 0$ K-band luminosity function, $\alpha_{\rm L} \approx -1$ (Cole et al. 2001), is much flatter than the low-mass slope of the dark halo mass function, $\alpha_{\rm M} \approx -2$ (Press & Schechter 1974). Therefore a crucial ingredient of any successful galaxy formation model is strong negative feedback to quench the formation of small galaxies (White & Frenk 1991; Benson et al. 2003). GALFORM incorporates this and other effects with a set of rules, each with an associated set of parameters. Some of these have a large effect on the properties of early galaxies, others mostly affect the present-day galaxy population. Recent studies using GALFORM have concentrated on two different variants, that of Baugh et al. (2005) (hereafter BAUGH05) and of Bower et al. (2006) (hereafter BOWER06), which adopt somewhat different prescriptions for star formation, feedback and the IMF (see also Lacey et al. (2008) for more details about the BAUGH05 model). The BAUGH05 model includes superwinds (following Benson et al. 2003) in order to better reproduce the bright end of the optical and near-IR galaxy luminosity function at $z = 0$, while the BOWER06 model instead accomplishes this by including feedback from accreting black holes (see also Croton et al. 2006). The other most important difference between the two models is that the BAUGH05 model assumes that stars form with a top-heavy IMF in starbursts, and a normal solar neighbourhood IMF in galaxy discs, while the BOWER06 model instead assumes that all star formation occurs with a solar neighbourhood IMF. In addition to this, the two models make somewhat different assumptions about the star formation time-scale in discs, supernova feedback, the time-scale for ejected gas to be re-incorporated into haloes and the triggering of starbursts.

While the BAUGH05 and BOWER06 models predict similar galaxy luminosity functions at optical and near-IR wavelengths at $z = 0$, the BAUGH05 model is in much better agreement with the observed numbers of star-forming galaxies seen at high redshifts, selected either as Lyman-dropouts or from their sub-millimetre emission (Baugh et al. 2005; Lacey et al. 2010a). As we will show later, the BAUGH05 model also predicts higher ionizing emissivities at high redshifts than the BOWER06 model, and a correspondingly higher redshift of reionization, in better agreement with current observational constraints. For these reasons, we concentrate in this paper on predictions from the BAUGH05 model. Not surprisingly, neither superwinds nor active galactic nuclei (AGN) greatly affect the predictions for galaxies at $z \gtrsim 6$, since the massive galaxies that are affected by these processes are extremely rare at such early times. Nevertheless, we do find quite significant differences between these two popular GALFORM variants in what they predict for ionizing emissivities at $z \gtrsim 6$, which are related to their different assumptions about star formation, supernova feedback and the IMF. We now discuss the physical processes incorporated in the BAUGH05 version of GALFORM model that have a large effect on $z \gtrsim 6$ galaxies, and why they were introduced in the original model.

2.1 Star formation

The model assumes two distinct modes of star formation, *quiescent* star formation in galaxy discs and *starbursts* triggered by galaxy mergers. In both cases the instantaneous star formation rate is parametrized as

$$\psi = \frac{M_{\rm cold}}{\tau_\star}, \qquad (1)$$

where $M_{\rm cold}$ is the amount of cold gas in the galaxy and $\tau_\star$ the star formation time-scale. Neglecting the lifetimes of massive stars (the instantaneous recycling approximation), the stellar mass in long-lived stars then builds up at a rate

$$\dot{M}_\star = (1 - R)\psi, \qquad (2)$$

where R is the recycling fraction; see Cole et al. (2000) for more details.

In the *quiescent star formation mode*, $\tau_\star$ depends on the circular velocity, $V_{\rm disc}$, of the galactic disc at the half-mass radius, as $\tau_\star = \tau_{\star,0}(V_{\rm disc}/200\,{\rm km\,s^{-1}})^{\alpha_\star}$, with $\tau_{\star,0} = 8$ Gyr and $\alpha_\star = -3$. This parametrization yields reasonable gas masses and star formation rates at low redshifts $z \sim 0$, and implies that ψ is quite low at high redshifts. This makes the high-z discs gas rich, so that when galaxies merge, there is a large reservoir of gas available for fueling a starburst (Baugh et al. 2005). *Bursts of star formation* are assumed to be triggered by galaxy mergers under certain conditions. The model includes both *major* and *minor* mergers, distinguished by the mass ratio of merging galaxies. Major mergers between spirals are assumed to destroy both discs and consume the remaining gas in a starburst. Minor mergers were introduced in the model motivated by the simulations of Hernquist & Mihos (1995); such a merger does not destroy the disc, but does build up the bulge. The star formation time-scale in the burst mode is shorter than in the quiescent mode (see Baugh et al. 2005).

The stellar initial mass function for quiescently forming stars is assumed to be similar to what is observed in the solar neighbourhood, specifically that proposed by Kennicutt (1983), ${\rm d}N/{\rm d}\ln(m) \propto m^{-x}$, with $x = 0.4$ for $m < 1\,{\rm M}_\odot$ and $x = 1.5$ for $m > 1\,{\rm M}_\odot$, However, in bursts the IMF is assumed to be top heavy, $x = 0$. In both cases, the IMF covers the mass range $0.15 < m/{\rm M}_\odot < 120$.

Star formation with a top-heavy IMF in bursts triggered by gas-rich galaxy mergers results in large UV luminosities from the massive young stars, and also the production of large quantities of metals and dust from supernovae. This dust in turn absorbs the copious UV radiation and re-radiates it at far-IR wavelengths. Both the frequent bursts at high redshifts and the top-heavy IMF are needed to boost the number of very luminous high-z IR galaxies to a level consistent with the observed number counts and redshift distribution of sub-millimetre galaxies. The parameters in the BAUGH05 model were chosen to match this sub-millimetre data, while at the same time yielding good fits to the Lyman-break galaxy luminosity function at $z \sim 3$, and remaining consistent with observational constraints at $z = 0$ (Baugh et al. 2005). The case for a top-heavy IMF for the formation of at least a fraction of stars is further supported by the fact that its use during starbursts also results in better agreement with observed metallicities (including α/Fe ratios) in intracluster gas in clusters and stars in elliptical galaxies (Nagashima et al. 2005a,b). Other independent observational evidence for variations in the IMF is discussed in Lacey et al. (2010a,b). We emphasize that our results do not depend crucially on the precise form of the top-heavy IMF assumed – similar results would be obtained for an IMF in which the high-mass slope was fixed but the low-mass turnover was varied, as proposed by Larson (1998). We will show below that the bursts, and the associated change in the IMF during bursts, *both* have large effects on the emissivity of ionizing photons by GALFORM galaxies at $z \gtrsim 6$.

2.2 Supernova feedback

The fact that galaxies in low-mass haloes form stars very inefficiently is likely due to energy injection from supernovae (Dekel &

Silk 1986). In the BAUGH05 model this is implemented by ejecting gas out of a galaxy disc at the rate of

$$\dot{M}_{\rm eject} = \psi \left(\frac{V_{\rm disc}}{V_{\rm hot}} \right)^{-\alpha_{\rm hot}}, \quad (3)$$

so that it is no longer available for star formation. Here, $V_{\rm disc}$ is the circular velocity of the galactic disc at the half-mass radius. Values of $V_{\rm hot} = 300$ km s^{-1} and $\alpha_{\rm hot} = 2$ were chosen to reproduce the faint-end slope of the *B*-band galaxy luminosity function at $z = 0$ (Baugh et al. 2005). Such strong feedback also significantly quenches star formation in small haloes at $z \gtrsim 6$, and therefore has a large impact on reionization. Note that the BOWER06 model incorporates even stronger SN feedback in small haloes.

2.3 Photoionization feedback

Star formation in small galaxies may be quenched as the IGM becomes ionized, either because cooling is suppressed (Efstathiou 1992), or because the higher IGM gas pressure inhibits gas from falling into haloes (Gnedin 2000b), or because photo-heating causes small galaxies to lose their gas (Hoeft et al. 2006; Okamoto, Gao & Theuns 2008). These effects may lead to a global suppression of star formation during and after the EoR, as seen in the simulations of Crain et al. (2009). The standard approach in GALFORM is to model this by suppressing the cooling of halo gas on to the galaxy when the host halo circular velocity is below a threshold value,

$$V_{\rm circ} < V_{\rm cut}, \quad (4)$$

at redshifts $z < z_{\rm cut}$ [but see also Benson et al. (2002a) for a more detailed treatment].

The default value of $V_{\rm cut} = 60$ km s^{-1} in the BAUGH05 model, originally guided by the results of Gnedin (2000b), is considerably larger than values found from more recent simulations (Hoeft et al. 2006; Okamoto et al. 2008). The original BAUGH05 model also assumed $z_{\rm cut} = 6$. Interestingly, because only the *gas cooling* in the halo is suppressed in GALFORM, a small galaxy with circular velocity $V < V_{\rm cut}$ can continue to form stars until it has exhausted its supply of *cold* (i.e. already cooled) gas. This way of suppressing galaxy formation in small haloes once the IGM is ionized has consequences for reionization and also for the luminosity function at later times, as we show below.

2.4 Modelling Lyman-continuum and broad-band SEDs

The GALFORM code computes the spectral energy distribution (SED) of each galaxy, given its star formation history and abundance evolution. The population synthesis models are based on the Padova stellar evolution tracks combined with Kurucz model atmospheres (Bressan, Granato & Silva 1998). The dust extinction is modelled with a prescription described by Cole et al. (2000) with improvements described in Lacey et al. (2010a). Convolving the SED with a filter response yields broad-band luminosities for the galaxy. Below we will use the rest-frame 1500-Å broad-band AB magnitudes of GALFORM galaxies to compare against observed galaxy luminosity functions at approximately the same rest-frame wavelength, after rescaling observed luminosities and number densities to the same MILLENNIUM cosmology as assumed in the model.

GALFORM also computes the Lyman-continuum luminosity for each galaxy, expressed as the emission rate of ionizing photons,

$$\dot{N}_{\rm LyC} = \int_{\nu_{\rm thresh}}^{\infty} \frac{L_\nu}{h\nu} \, {\rm d}\nu \, , \quad (5)$$

where L_ν is the SED of the galaxy and $\nu_{\rm thresh}$ is the Lyman-limit frequency, $h\nu_{\rm thresh} = 13.6$ eV. Note that the number of ionizing photons produced per solar mass of stars formed is very different for the Kennicutt IMF assumed during quiescent star formation compared to the top-heavy IMF in bursts ($N_{\rm LyC}/M_\star = 3.2 \times 10^{60}$ and 3.5×10^{61}, respectively, for solar metallicity).

A considerable fraction of those ionizing photons may be absorbed locally in the interstellar medium of the galaxy or by gas in the surrounding halo, and the fraction $f_{\rm esc}$ of photons that does manage to escape into the IGM is very uncertain. Observations of $z \sim 3$–4 Lyman-break galaxies (LBGs) by Steidel, Pettini & Adelberger (2001) and Shapley et al. (2006) suggest $f_{\rm esc} \sim 0.01$–0.1 or even lower (Giallongo et al. 2002) (but note the slightly different definition of $f_{\rm esc}$ there). The escape fraction may depend strongly on the porosity of the interstellar medium within the galaxy or the presence of supernova-driven winds (e.g. Ciardi, Bianchi & Ferrara 2002; Clarke & Oey 2002). Some of the more recent models that attempt to include these effects suggest that $z \gtrsim 6$ galaxies may have significantly larger escape fractions, $f_{\rm esc} \sim 0.5$ (e.g. Wise & Cen 2009; Razoumov & Sommer-Larsen 2010). Note that this parameter is unlikely to be independent of metallicity, gas content and halo mass. In this paper, we simply assume $f_{\rm esc}$ to be the same for all galaxies.

We will now discuss the net emissivity of ionizing photons in the BAUGH05 model, and how that depends on GALFORM parameters.

3 IONIZING EMISSIVITIES

The emissivity $\epsilon(z)$, the number of ionizing photons produced per unit comoving volume at redshift z, is found by summing the Lyman-continuum luminosity of all galaxies, per unit volume,

$$\epsilon(z) = \int_0^{\infty} \dot{N}_{\rm LyC} \, \Phi(\dot{N}_{\rm LyC}) \, {\rm d}\dot{N}_{\rm LyC}, \quad (6)$$

where $\Phi(\dot{N}_{\rm LyC})$ is the Lyman-continuum luminosity function. The emissivity $\epsilon(z)$ increases by approximately 1.5 dex between $z = 13$ and $z = 5$ in the BAUGH05 model (Fig. 1, thin line), mostly as a consequence of evolution in the halo mass function, as we will show below.

Integrating $\epsilon(z)$ down to a given redshift yields the total number of ionizing photons produced per unit comoving volume up to that time. This number can be compared to the mean comoving number density of hydrogen atoms, $n_{\rm H}$. Reionization will occur when their ratio

$$\mathcal{R}(z) \equiv \frac{\int_\infty^z \epsilon(z) \, {\rm d}z}{n_{\rm H}} \quad (7)$$

is $\mathcal{R} = (1 + N_{\rm rec})/f_{\rm esc}$. Here, $N_{\rm rec}$ denotes the mean number of recombinations per hydrogen atom up to reionization and $f_{\rm esc}$ is the mean escape fraction from Section 2.4.

Estimating $N_{\rm rec}$ is not straightforward. Recombinations can occur in the higher-density regions of the general IGM, in 'mini-haloes' that have too shallow potential wells for star formation (Shapiro, Iliev & Raga 2004; Ciardi et al. 2006) or in even higher-density regions associated with Lyman-limit or damped Lyman α systems. The value of $N_{\rm rec}$ will itself depend on $\int_\infty^z \epsilon(z) \, {\rm d}z$, since a slower build-up of the ionization rate will allow more time for recombinations. Interestingly, once the IGM is ionized, the smoothing of the density field due to gas pressure following photo-heating reduces the recombination rate (Pawlik, Schaye & van Scherpenzeel 2009). Current simulations of the EoR suggest values of $N_{\rm rec}$ of a few (Iliev et al. 2006; McQuinn et al. 2007; Trac & Cen 2007).

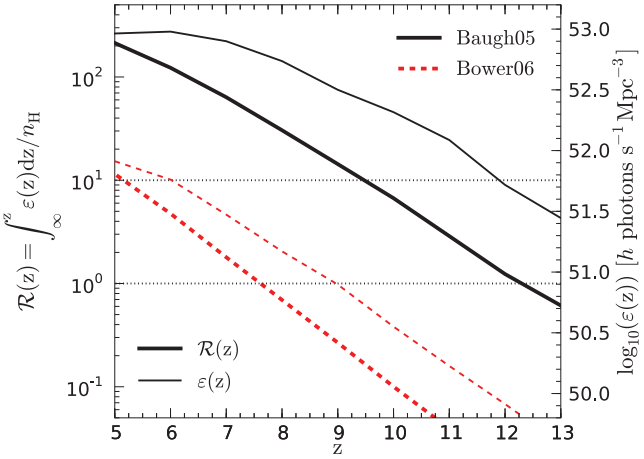

Figure 1. The ratio $\mathcal{R}(z)$ of the number of ionizing photons produced per hydrogen atom up to redshift z in the two fiducial GALFORM models, BAUGH05 and BOWER06 (thick lines, left y-axis) as well as the total emissivity, $\epsilon(z)$, in the same models (thin lines, right y-axis). The horizontal dashed lines mark the minimum number of photons per H atom that must be produced to achieve reionization: in the most optimistic case, only one (bottom line), but 10 or more when reasonable values for the ionizing escape fraction and mean number of recombinations per H atom are taken into account (top line). The BAUGH05 model produces ∼100 times more ionizing photons by $z \sim 10$ than BOWER06 and reaches 10 photons per H atom $\Delta z \sim 5$ earlier. The decreased slope in $\epsilon(z)$ at $z \leq 6$ is caused by the turn-on of photoionization feedback at $z = 6$ in both models.

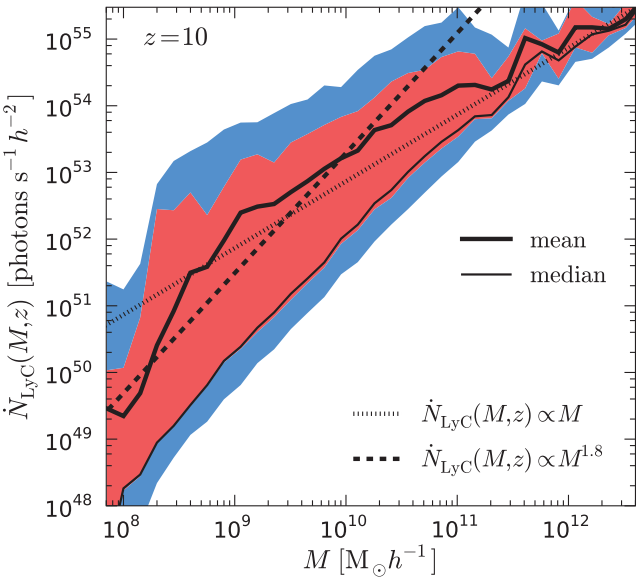

Figure 2. Lyman-continuum photon luminosity, $\dot{N}_{\mathrm{LyC}}(M, z)$, of haloes as a function of halo mass M, in the BAUGH05 model at $z = 10$ (median and mean relation are shown as thick and thin solid lines, respectively). $\dot{N}_{\mathrm{LyC}}$ increases approximately as $\dot{N}_{\mathrm{LyC}} \propto M^{1.8}$ for small haloes $M \lesssim 2 \times 10^9\, h^{-1}\,\mathrm{M}_{\odot}$, and as $\dot{N}_{\mathrm{LyC}} \propto M$ for more massive haloes, with little dependence on redshift. The 50 and 90 per cent ranges of $\dot{N}_{\mathrm{LyC}}(M)$ at given halo mass are shaded red and purple, respectively. There is up to 5 dex range in $\dot{N}_{\mathrm{LyC}}$ at a given mass, a consequence of the dominance of starbursts in producing ionizing photons.

Combining the estimate of $1 + N_{\mathrm{rec}} \sim 2$ with a reasonable escape fraction of $f_{\mathrm{esc}} \sim 0.2$ then suggests that reionization requires a value of $\mathcal{R} \sim 10$. This is plotted as a function of redshift for the default values of the BAUGH05 and BOWER06 GALFORM parameters in Fig. 1 (thick lines), suggesting that the BAUGH05 model will produce a reasonable reionization redshift $z_{\mathrm{reion}} \sim 10$, $\Delta z \sim 5$ before BOWER06. Next we discuss the properties of the galaxies and haloes that dominate the emissivity in the BAUGH05 model, and how strongly these depend on the assumed parametrization in the model, following the same order as given in Section 2.

3.1 Effect of star formation parameters and IMF

The number of ionizing photons produced per unit time by galaxies in a halo of given mass, $\dot{N}_{\mathrm{LyC}}(M, z)$, is plotted as a function of M in Fig. 2. The virial temperature T_{vir} of haloes with $M < M_{\mathrm{min}} \approx 10^8\, h^{-1}\,\mathrm{M}_{\odot}$ is too low to enable radiative cooling by atomic lines and hence such haloes do not form stars.[7] Given that $T_{\mathrm{vir}} \propto (1 + z)$ at fixed M, there is strong redshift dependence in $\dot{N}_{\mathrm{LyC}}(M, z)$ at very low masses, but above this minimum mass GALFORM predicts essentially no evolution in the mean $\dot{N}_{\mathrm{LyC}}(M, z)$ between $z = 15$ and $z = 6$, but with a modest ∼50 per cent decrease in the median in haloes with mass $M \gtrsim 10^{10}\, h^{-1}\,\mathrm{M}_{\odot}$ in the same redshift range.

The mean $\dot{N}_{\mathrm{LyC}}$ at a given halo mass increases approximately as $\dot{N}_{\mathrm{LyC}} \propto M^{1.8}$ for small haloes $M \lesssim 2 \times 10^9\, h^{-1}\,\mathrm{M}_{\odot}$, and roughly as $\dot{N}_{\mathrm{LyC}} \propto M$ for more massive haloes, in contrast to many recent simulations of reionization which assume a simple $\dot{N}_{\mathrm{LyC}} \propto M$ relation for all M (e.g. Furlanetto et al. 2004; Iliev et al. 2006). Interestingly, there is a very large difference between the mean and median of $\dot{N}_{\mathrm{LyC}}$ at given M, and there is also a very large range, up to ∼5 dex, in $\dot{N}_{\mathrm{LyC}}$ at *given* M (Fig. 2). Both are consequences of the importance of bursts in generating ionizing photons, as we will discuss in more detail below.

The total Lyman-continuum emissivity per dex in halo mass $\mathrm{d}\epsilon/\mathrm{d}\log_{10}(M)$ (Fig. 3), can be obtained by combining the mean luminosity of a single halo of given mass, $\dot{N}_{\mathrm{LyC}}(M)$, with the number of haloes of that mass, $\mathrm{d}n/\mathrm{d}\log_{10}(M)$. This function evolves rapidly as a consequence of the rapid build-up of more massive haloes as time progresses. The halo mass below which 50 per cent of ionizing photons are produced increases from $\sim 8 \times 10^8\, h^{-1}\,\mathrm{M}_{\odot}$ at $z = 14$ by an order of magnitude to $\sim 8 \times 10^9\, h^{-1}\,\mathrm{M}_{\odot}$ at $z = 6$ (top panel of Fig. 3). At high z, the mass range of haloes that contribute significantly to ϵ is relatively small, of order 1 dex, since it is limited at low M by M_{min} and at large M by the exponential drop in the abundance of more massive haloes. At later redshift $z \sim 6$, $\mathrm{d}\,\epsilon/\mathrm{d}\log_{10}M$ is nearly independent of M over nearly 2 dex, a consequence of the fact that the ionizing photon luminosity of haloes increases with halo mass approximately as $\dot{N}_{\mathrm{LyC}}(M) \propto M^1$ (dotted line in Fig. 2), whereas the number density of haloes decreases with increasing mass approximately as $\mathrm{d}n/\mathrm{d}\log_{10} M \propto M^{-1}$.

The impact of starbursts on the emissivity is quantified in Fig. 4. In the default BAUGH05 model, bursts increase the ionizing emissivity relative to that from quiescent galaxies both as a consequence of the reduction in star formation time-scale, equation (1), and because of the assumed change to a top-heavy IMF. The net effect is a factor of 5–10 increase in ϵ depending on redshift, with approximately 65 per cent of the increase due to bursts following a minor merger. Most of the increase in $\dot{N}_{\mathrm{LyC}}$ is a consequence of the assumed change in IMF.

Neglecting bursts does not affect the 'characteristic' halo mass below which 50 per cent of the ionizing photons are produced

[7] We recall that this GALFORM model does not consider Pop. III stars that form due to molecular cooling in such small haloes.

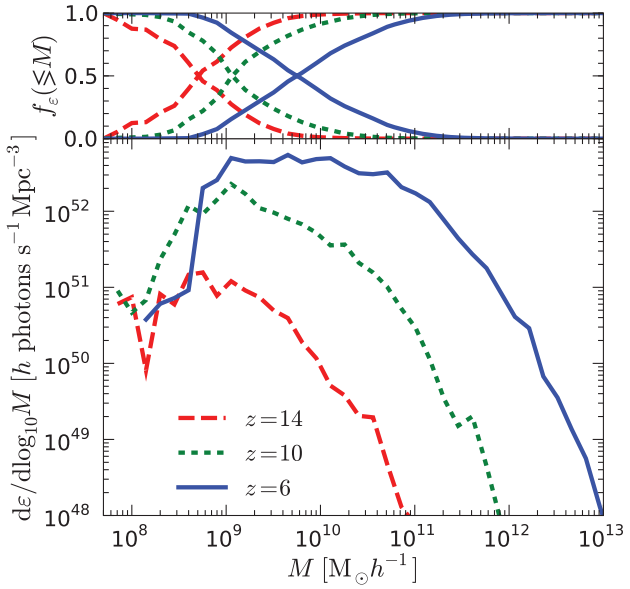

Figure 3. Main panel: Lyman-continuum emissivity as a function of halo mass, $\mathrm{d}\epsilon(M, z)/\mathrm{d}\log_{10}(M)$, for various redshifts indicated in the panel. The emissivity, which is low for very low mass haloes that are unable to cool gas, reaches a peak which increases with decreasing z, and a tail towards larger masses is set by the exponential drop in the number of massive haloes. At $z \sim 10$ most ionizing photons are produced by haloes in a relatively small mass range, $\sim$1 dex. Top inset: Cumulative fraction f_c of ionizing photons produced in haloes more massive or less massive than a given value (rising and falling curves, respectively). The mass of haloes below which 50 per cent of ionizing photons is produced rises by approximately an order of magnitude from $\sim 8 \times 10^8\, h^{-1}\,\mathrm{M}_\odot$ at $z = 14$ to $\sim 8 \times 10^9\, h^{-1}\,\mathrm{M}_\odot$ at $z = 6$.

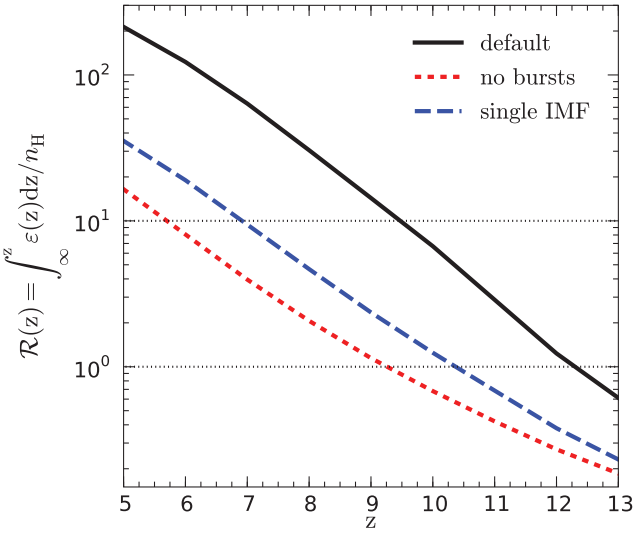

Figure 4. Dependence of the total number of ionizing photons produced per hydrogen atom up to redshift z, $\mathcal{R}(z)$, on the starburst parameters in Baugh05: default model (black), no bursts (red), including bursts, but not the change to a top-heavy IMF in bursts (blue). Including bursts increases $\epsilon(z)$ by a factor of 5–10, depending on redshift. The effect of the change in IMF in the bursts is large, yet even without it bursts still increase ϵ by a factor of $\sim$2. Neglecting bursts delays reionization ($\mathcal{R} = 10$) by $\Delta z \sim 4$.

(Fig. 5) but it does increase the range of halo masses responsible for the majority (e.g. 90 per cent) of ionizing photon production by $\sim$1 dex (compare solid black and short dashed red lines in the top inset of the same panel).

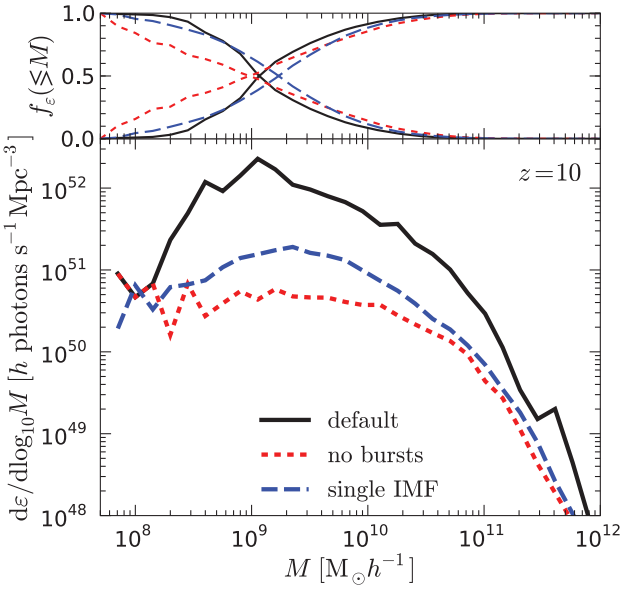

Figure 5. Dependence of emissivity as a function of halo mass, $\mathrm{d}\epsilon/\mathrm{d}\log_{10}M$, on the burst parameters in the Baugh05 model. The characteristic halo mass at which 50 per cent of the ionizing photons is produced does not greatly depend on the burst parameters. However, switching off the bursts (red short dashed line) extends the halo mass range in which the majority ($\sim$90 per cent) of ionizing photons is produced by $\sim$1 order of magnitude in comparison to the default model (solid black line).

Bursts skew the distribution of $\dot{N}_\mathrm{LyC}$ at given halo mass by introducing a long tail of much more luminous galaxies which happen to be bursting, with again the assumed change in IMF playing a dominant role (Fig. 6). These few, but relatively bright, galaxies dominate the emissivity at that halo mass by a large factor. Remarkably, there can be nearly a 5 dex range in Lyman-continuum luminosity at a given halo mass.

We conclude that bursts are a crucial ingredient in order for the Baugh05 model to produce that many ionizing photons by $z \sim 10$. Not only do stars form at a greater rate due to the decrease in the star formation time-scale, but especially the change to a top-heavy IMF in bursts, originally introduced to produce sufficiently luminous sub-millimetre galaxies at $z = 1$–3, and to produce sufficient metals by $z = 0$, causes a small fraction of galaxies to emit copious ionizing radiation. The bursts occur mostly due to minor mergers, and are so effective because the merging galaxies are very gas rich, itself a consequence of the inefficient star formation in their quiescent state. Bursts also introduce nearly 5 dex of scatter in the $\dot{N}_\mathrm{LyC}$–halo mass relation. These same bursts are also a crucial ingredient for reproducing the observed luminosity function of Lyman-break galaxies at $z > 6$, as shown in Lacey et al. (2010a) and also discussed below (Fig. 9). But first we investigate the effect of the feedback parameters on ϵ.

3.2 Effect of supernova feedback parameters

We consider two variants to the default Baugh05 supernova feedback parametrization to investigate how strongly they affect the emissivity of ionizing photons. The 'weak' feedback choice, shown in Fig. 7 (green dashed line), uses the parameters $(V_\mathrm{hot}, \alpha_\mathrm{hot}) = (100\,\mathrm{km\,s^{-1}}, 1)$ (as defined in equation 3), as opposed to the default Baugh05 values of $(300\,\mathrm{km\,s^{-1}}, 2)$. The ionizing emissivity of the weak feedback model is not very different from a model without

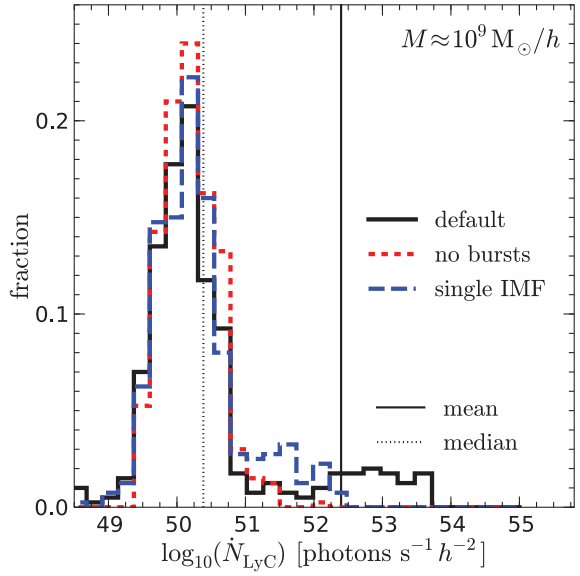

Figure 6. Distribution of Lyman-continuum photon luminosities, $\dot{N}_{\mathrm{LyC}}$ at $z = 10$, for haloes with mass $M \approx 10^9\ h^{-1}\,\mathrm{M}_\odot$. Different line styles refer to different models for the bursts, vertical dotted and solid lines indicate median and mean $\dot{N}_{\mathrm{LyC}}$ in the default model, respectively. The distribution of $\dot{N}_{\mathrm{LyC}}$ peaks at a few times $10^{50}\,h^{-2}$ photons s^{-1}, but allowing bursts introduces a long tail towards much more luminous galaxies (red versus black histograms), with the change in IMF in bursts having a large contribution to this (blue versus black histograms). This tail makes the mean $\dot{N}_{\mathrm{LyC}}$ nearly 2 dex brighter than the median. In the default model with a top-heavy IMF in bursts there is a nearly 5 dex range in luminosity at given halo mass.

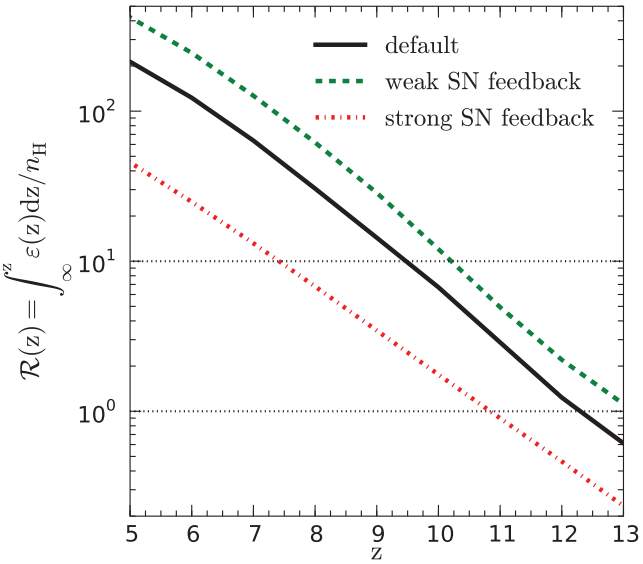

Figure 7. Dependence of the total number of ionizing photons produced per hydrogen atom up to redshift z, $\mathcal{R}(z)$, on the GALFORM parameters that govern supernova feedback. Decreasing the efficiency of SN feedback (green dashed line) doubles the production of ionizing photons, resulting in reionization occurring $\Delta z \sim 0.7$ earlier. Increasing feedback from supernovae to the values used in the BOWER06 model (red dot–dashed line) delays reionization by $\Delta z \sim 2$.

any SN feedback at all; it produces nearly twice as many ionizing photons as the default BAUGH05 model, increasing the reionization redshift, for which $\mathcal{R} = 10$, by $\Delta z \sim 0.7$. The 'strong' feedback model has $(V_{\mathrm{hot}}, \alpha_{\mathrm{hot}}) = (500\,\mathrm{km\,s^{-1}}, 3)$, close to the values (475 km s^{-1}, 3.2) used in BOWER06 ; this choice of parameters decreases $\epsilon(z)$ by a factor of $\sim$5, delaying reionization by $\Delta z \sim 2$.

Even stronger feedback is probably ruled out by the comparison with the observed $z = 6$ Lyman-break far-UV luminosity function (LF) discussed in Fig. 10 below, but all three models are probably equally consistent with the $z = 10$ LF. This is not surprising since the SN parameters affect mostly the fainter galaxies that are currently below the detection limits at these very high redshifts. We note that the standard approach in GALFORM modelling is to constrain the SN feedback parameters by comparison with galaxy properties at $z = 0$. However, even if one chooses to relax the $z = 0$ constraints on the SN feedback, on the grounds that SN feedback might operate differently in early galaxies, the constraints on this from the $z \geq 6$ Lyman-break LFs still limit the uncertainty in ϵ to a factor of $\sim$2 in the BAUGH05 model.

3.3 Effect of photoionization feedback parameters

As discussed in Section 2.3, the effect of photoionization feedback from reionization on galaxy formation is modelled in GALFORM with a simple prescription, whereby gas cooling is suppressed in all haloes of circular velocity $V_{\mathrm{circ}} < V_{\mathrm{cut}}$ after the reionization redshift z_{cut}, equation (4). The key feature of this prescription is that the cold gas already present in galaxies before the onset of photoionization feedback is allowed to form stars after z_{cut}. This results in a significant delay between the time at which the surroundings of the galaxy become ionized and the quenching of star formation. This is in contrast to several current simulations of reionization, which assume that suppression is instantaneous (e.g. Iliev et al. 2006). The delay is in fact so large that the suppression of star formation (and hence also the production of ionizing photons) due to photoionization has little effect on the progression of reionization, as we will show elsewhere.

However, given enough time, photoionizing feedback does have a strong effect on the ionizing emissivity, as shown in Fig. 8. Note that the default BAUGH05 model uses a value of $V_{\mathrm{cut}} = 60\,\mathrm{km\,s^{-1}}$ which is unrealistically high compared to more recent simulation results, which reduces ϵ by as much as 50 per cent by redshift 5 compared to the no-reionization model (assuming reionization occurs at $z_{\mathrm{cut}} = 10$). The more modern value of $V_{\mathrm{cut}} \sim 30\,\mathrm{km\,s^{-1}}$, suggested by the simulations of Okamoto et al. (2008), yields a smaller yet still significant decrease in the total emissivity at $z = 5$ of 15 per cent.

We conclude that photoionization suppression as implemented in GALFORM has little effect on the production of ionizing photons until well after reionization, but it does affect the emissivity at later times. Interestingly, the photoionization quenching of star formation also has observable effects on the Lyman-break LF, as we discuss in more detail below (Fig. 11).

4 FAR-UV LUMINOSITY FUNCTIONS OF THE GALAXIES THAT CAUSED REIONIZATION

The Lyman-break colour-selection technique has proven to be very effective for identifying large samples of star-forming galaxies at high redshifts since its first application at $z \sim 3$ (Steidel et al. 1996). This selection method was first applied at $z \sim 6$ by Bouwens et al. (2003), and recent deep near-IR imaging with *Hubble Space Telescope* (*HST*) has been used to discover significant numbers of candidate Lyman-break galaxies (LBGs) at $z \sim 7$–8, and a few candidates at $z \sim 10$ (Bouwens et al. 2007; Bunker et al. 2009a; Bouwens et al. 2009, 2010; Oesch et al. 2009). We therefore now

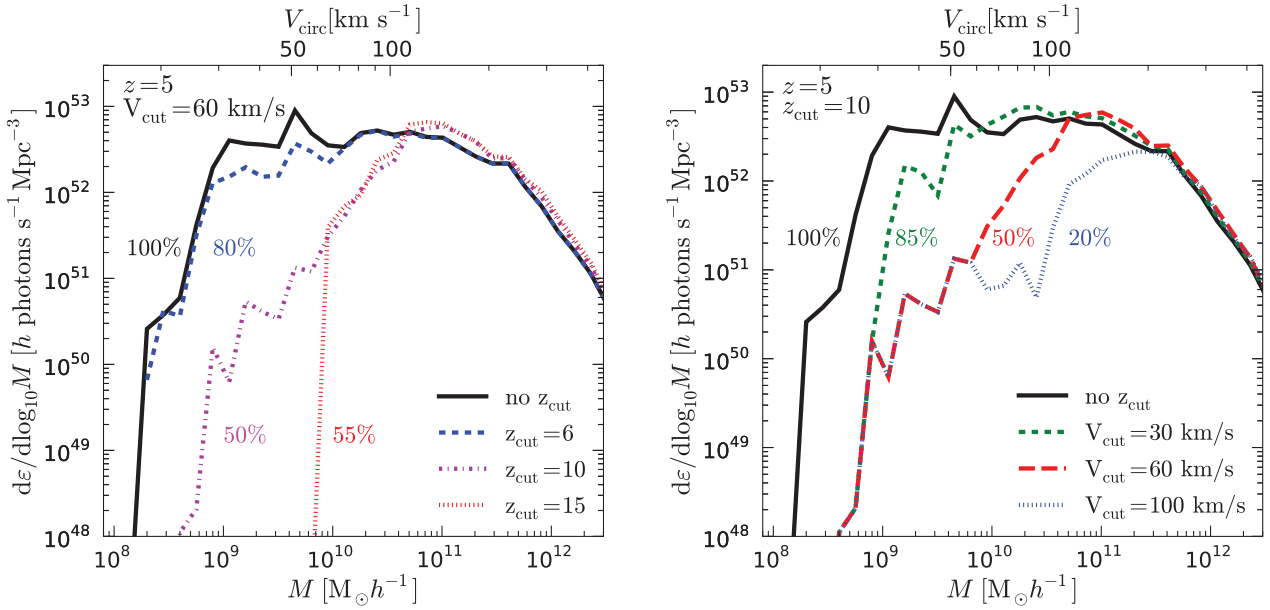

Figure 8. Dependence of Lyman-continuum emissivity as a function of halo mass, $\mathrm{d}\epsilon/\mathrm{d}\log_{10}M$, at redshift $z = 5$, on the GALFORM parameters that describe photoionization feedback. Left-hand panel: Dependence on the reionization redshift $z_{\rm cut}$ (indicated in the legend; 'no $z_{\rm cut}$' assumes reionization occurs below $z = 5$) below which the IGM is assumed to be fully ionized. The impact of photoionization suppression takes a long time to take effect, but when suppression sets in it dramatically reduces the Lyman-continuum (LC) luminosity of the galaxies. Right-hand panel: Dependence on the circular velocity $V_{\rm cut}$ below which photoionization feedback affects the galaxy. The suppression in $\mathrm{d}\epsilon/\mathrm{d}\log_{10}M$ becomes evident at circular velocities below $\sim 2V_{\rm cut}$. The scale on top of both panels gives the circular velocity of the haloes (in km s^{-1}) at $z = 5$. The numbers next to the lines give the ratio of the total emissivity of that model compared to the model with no photoionization feedback (black lines).

have direct detections of a part of the galaxy population responsible for reionizing the Universe at $z \sim 6$–10. The companion paper by Lacey et al. (2010a) presents a detailed comparison of the predictions of GALFORM models with observations of Lyman-break galaxies over the whole redshift range $z = 3$–10, including rest-frame far-UV luminosity functions, sizes, masses and other properties. In this section, we investigate what constraints can be put on the GALFORM parameters to which the emissivity of ionizing photons ϵ is particularly sensitive from observations of the rest-frame far-UV (1500 Å) luminosity functions of $z \sim 6$–10 Lyman-break galaxies alone. We also investigate the extent to which the currently observed Lyman-break galaxies contribute to the total emissivity of ionizing photons, according to the GALFORM model.

4.1 Effect of star formation parameters and IMF

The rest-frame 1500-Å broad-band GALFORM LFs at $z = 6$ and $z = 10$ are compared against the *HST* data on LBGs in Fig. 9. The default BAUGH05 model reproduces the LFs at both redshifts, a considerable success. Clearly, starbursts are crucial for bringing the 1500-Å luminosities of the galaxies to the observed levels (compare the red short dashed lines for the model without bursts with the other two lines). These same bursts also produce the bulk of the ionizing photons, as we showed in Fig. 5.

Interestingly, both the model with a top-heavy IMF in bursts (the default model, black lines), and a model which uses the same Kennicutt (1983) IMF in both quiescent galaxies and bursts (blue dashed lines) fit the observed LFs nearly equally well at these redshifts, notwithstanding the significant differences between these models that we pointed out in, for example, Fig. 4. The reason for this is dust extinction: the default model with the top-heavy IMF produces more metals and hence also more dust as compared to the Kennicutt (1983) IMF, and the larger dust extinction partly compensates the larger intrinsic far-UV luminosities (see Lacey et al. 2010a, for more details). Previously we found that a change in IMF affected the ionizing emissivity considerably (Fig. 4), but there we assumed that the escape fraction of ionizing photons, $f_{\rm esc}$, is simply a constant. A physically motivated $f_{\rm esc}$ would presumably depend on galactic dust content, reducing the difference between the top-heavy IMF and single IMF emissivities (see e.g. Benson et al. 2006) which would shift the completion of reionization we found here to lower redshifts. We will examine these issues in future work.

The currently detected candidate LBGs contribute only a small fraction of the total emissivity of the whole population of galaxies predicted by GALFORM at high z. Even at $z \sim 6$ (top panel), galaxies brighter than the current observational limit ($M_{1500,\rm AB,min} \sim -18$) contribute only ∼40 per cent of the total ionizing emissivity (solid black line in the top inset). If a single Kennicutt (1983) IMF is assumed, that fraction is even lower (∼20 per cent; long dashed blue line). At $z \sim 10$ (bottom panel), more than 90 per cent of ionizing photons are emitted by galaxies below the current detection limit for the default BAUGH05 parameters, and for a single IMF model that fraction is ∼95 per cent.

The BAUGH05 model predicts that the galaxies that produce the bulk of the ionizing photons at $z \sim 10$ are intrinsically faint, with 50 per cent of ionizing photons produced in galaxies fainter than $m_{\rm AB} \sim 31$ in the H-band. Clearly, it will be challenging to detect a significant fraction of the galaxies that emit the photons that reionized the Universe, even with the *James Webb Space Telescope* (*JWST*); see e.g. the *JWST* white paper by Stiavelli et al.[8]

[8] http://www.stsci.edu/jwst/science/whitepapers/

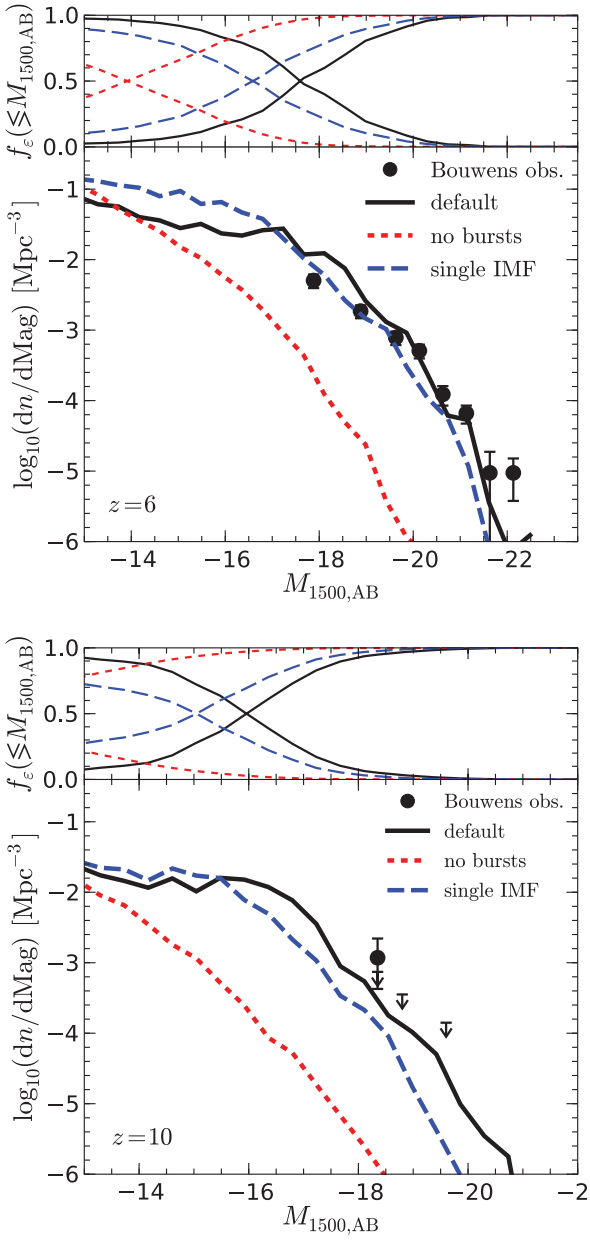

Figure 9. Rest-frame 1500-Å broad-band luminosity functions of the default Baugh05 model (lines) compared to data from Bouwens et al. (2007) and Bouwens et al. (2009), at redshifts $z = 6$ and 10 (symbols with error bars; downward pointing arrows mark 1σ upper limits). Both the default Baugh05 model (black solid lines) and the single IMF variant (long dashed blue lines) produce reasonable fits to the observed LFs at both redshifts. The *insets* in each panel show the cumulative fraction of ionizing photons produced in galaxies brighter than, or fainter than, a given value of the $M_{1500,\mathrm{AB}}$ absolute AB magnitude (rising and falling curves, respectively).

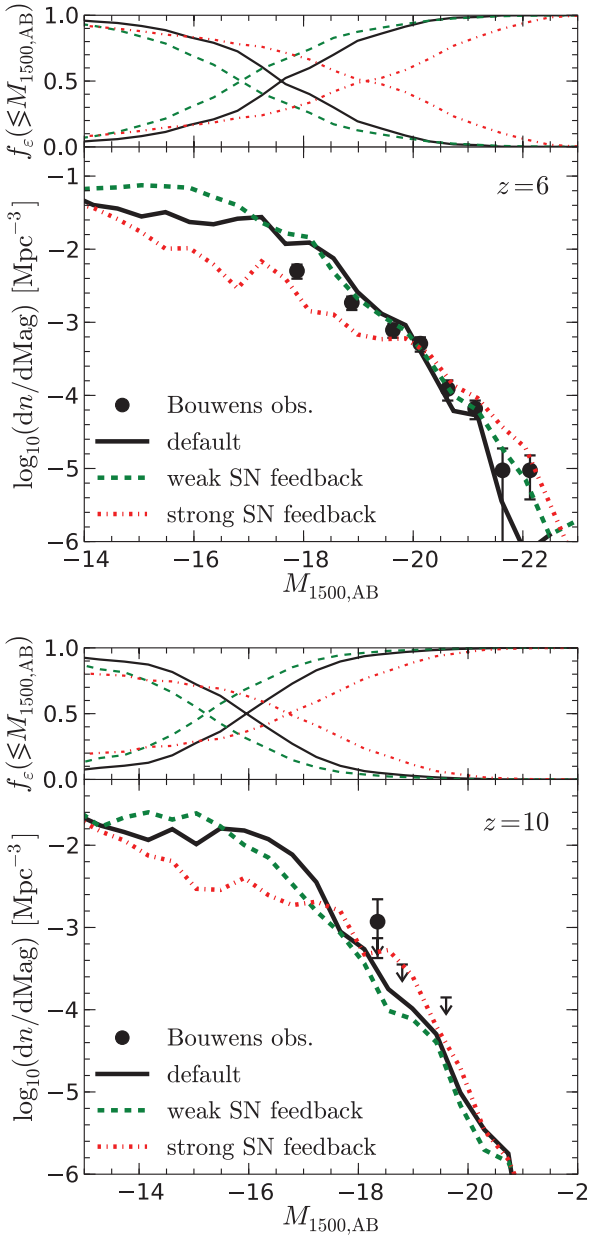

Figure 10. The effect of the supernova feedback parameters on the predicted rest-frame 1500-Å luminosity functions in the Baugh05 model at redshifts 6 (top) and 10 (bottom), and models with weaker and stronger feedback (green and red lines, respectively); the corresponding emissivities were shown Fig. 7. The data (solid points) are from Bouwens et al., as in Fig. 9. The weak feedback model (green dashed line) slightly overpredicts the number of galaxies at $z \sim 6$, and the strong feedback model underpredicts the numbers. However at $z \sim 10$ the bright, observed end of the LF is equally well fit by all models.

4.2 Effect of supernova feedback parameters

The strength of supernova feedback cannot be strongly constrained with the current $z \gtrsim 6$ data (Fig. 10; see also Lacey et al. 2010a). At the lowest redshift ($z = 6$; top panel), the faint end currently probed provides some constraints on the strength of the supernova feedback, with the weak and strong models on either side of the data. However, the $z = 10$ data only probe the very brightest galaxies, for which all three models predict very similar LFs.

Of course, the supernova feedback parameters in GALFORM are strongly constrained by even lower redshift data. However, the reader should keep in mind that the emissivities we predict here are contingent on the assumption that the basic physics of galaxy formation (in particular the impact of supernova feedback on regulating star formation) is the same at all redshifts. If for some reason this is not true, the currently available observations at $z \gtrsim 6$ do not probe sufficiently faint galaxies to determine the impact of supernova feedback on the total emissivity produced by all galaxies.

4.3 Effect of photoionization feedback parameters

As discussed in Section 2.3, the high-z 1500-Å LF may hold information about the reionization history, if star formation in galaxies is quenched once their surroundings are ionized. This is illustrated in Fig. 11. The $z = 6$ LF is reasonably well fit by the default BAUGH05 model, which assumes that reionization occurs at $z_{\rm cut} = 6$ (and hence for which there is no suppression in Fig. 11).

However, recent CMB measurements of the Thomson scattering optical depth suggest reionization at $z \sim 10$, assuming an instantaneous reionization model (Komatsu et al. 2010). The GALFORM model with such early reionization and $V_{\rm cut} = 60$ km s^{-1} underpredicts the faint end of the observed $z = 6$ luminosity function by a considerable amount, a factor of ∼4 for galaxies with $M_{1500,\rm AB}$ fainter than −18. Clearly, photoionization suppression is then too strong. But we already argued that the default value of the halo circular velocity below which galaxies are affected by photoionizing feedback ($V_{\rm cut} = 60$ km s^{-1}) is too high, with the hydrodynamical simulations of Okamoto et al. (2008) suggesting a much lower value of $V_{\rm cut} = 30$ km s^{-1}. With this lower value of $V_{\rm cut}$, the LF at $z = 6$ is in good agreement with the data, even for an early reionization redshift [green dotted line; see also Lacey et al. (2010a)]; in fact this model fits the $z = 6$ data best. Noting that the CMB data are the strongest current constraint on reionization, we argue that this result gives an *observational constraint* on the characteristic strength of photoionization feedback that strengthens the conclusion from current simulations.

The far-UV luminosity functions predicted by the BAUGH05 model and presented here and in Lacey et al. (2010a) show a very good agreement with the $z \gtrsim 6$ data of Bouwens et al. (2007, 2008, 2009, 2010). This is a significant success for a model for which the parameters were chosen to match much lower redshift data, and provides us with reasonable confidence in using the ionizing luminosities predicted by this model in future, more detailed modelling of the reionization process (Raičević et al. 2010).

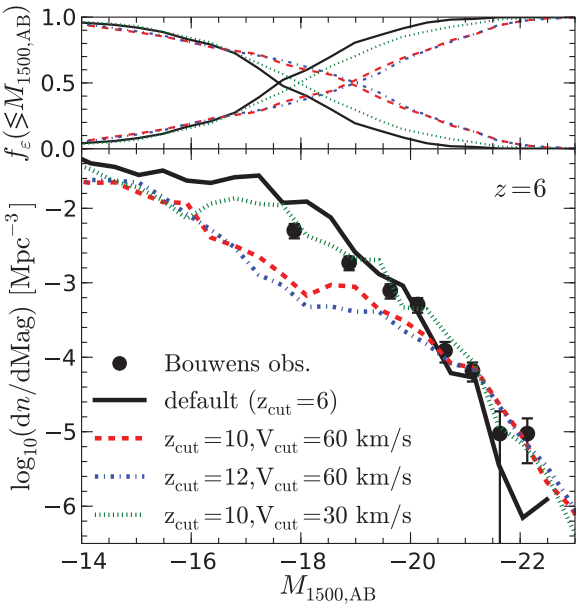

Figure 11. The effect of photoionization on the predicted rest-frame 1500-Å LF in the BAUGH05 model at redshift 6. The models differ in their choice of reionization redshifts ($z_{\rm cut}$), and of the halo circular velocity below which galaxies are affected by photoionizing feedback ($V_{\rm cut}$). The corresponding emissivities were shown in Fig. 8. The data (solid points) are from Bouwens et al., as in Fig. 9. If galaxies with $V_{\rm cut} = 60$ km s^{-1} are affected by suppression, then early reionization ($z_{\rm cut} \sim 10$) can be ruled out by the current data, since then the predicted number density of galaxies at $M_{1500,\rm AB} \sim -18$ is ∼4 times lower than observed (red lines). A more reasonable suppression scale of $V_{\rm cut} = 30$ km s^{-1} is consistent with early reionization (green lines).

We have seen that the BAUGH05 model predicts that the bulk of ionizing photons is produced by galaxies significantly below the current detection limit. It is a common practice to fit observed LFs with a Schechter function, and use the fit to extrapolate the LF to fainter galaxies. We show in the Appendix that this approach can lead to significant errors in estimating the total emissivity, since the LFs predicted by GALFORM deviate significantly from Schechter functions in some ranges of luminosity, in particular due to the effects of bursts. As a result, the Schechter fit parameters depend significantly on the luminosity range over which the fit is done, and the total emissivity estimated by extrapolating this fit is sensitive to the minimum luminosity set by the observational detection limit.

5 CONCLUSIONS

We used the Baugh et al. (2005) version of the GALFORM galaxy formation model to compute the emissivity (ϵ) of hydrogen-ionizing photons in the redshift range relevant for reionization, $z \gtrsim 6$, and investigated the impact of changing some of the model parameters from their default values. A crucial element of this model is that mergers between gas-rich galaxies increase ϵ dramatically compared to a model without bursts, mainly due to the change to a top-heavy IMF in bursts assumed in the model. The Baugh et al. model, with the same parameter values as used here, has previously been shown to reproduce a wide range of observed galaxy properties at lower redshifts.

The main points presented in the paper are as follows.

(i) The BAUGH05 model produces enough ionizing photons to complete reionization by $z \sim 10$ with galaxies alone, assuming a reasonable photon consumption (two photons per hydrogen atom, allowing an average of one recombination per H atom) and a 20 per cent escape fraction of Lyman-continuum (LC) photons from galaxies (Fig. 1).

(ii) Starbursts are crucial for boosting the ionizing emissivity leading up to reionization. The majority of ionizing photons is produced in a relatively small fraction of galaxies at any given time that are bursting, and that are up to 5 dex brighter than non-bursting galaxies in haloes of the same mass. Such bursts also increase the importance of intermediate-mass haloes ($M \sim 10^9\,h^{-1}\,\mathrm{M}_\odot$) compared to simpler models that do not include bursts (Fig. 4).

(iii) The top-heavy IMF used in the burst star formation mode is the main factor making the bursts so luminous, with ∼10 times as many ionizing photons emitted per solar mass of stars formed as compared to the Kennicutt (1983) IMF. The change to a top-heavy IMF in starbursts was previously introduced in the model to reproduce the sub-millimetre galaxy counts at lower redshifts ($z \sim$ 1–3), not the ionizing emissivity we discuss here, but it is crucial for completing reionization in agreement with current observational constraints. The model with a single IMF reionizes $\Delta z \sim 2.5$ later than the default model (Fig. 4).

(iv) The assumed strength of supernova feedback has a strong impact on the ionizing emissivity, because the galaxies that dominate ϵ reside in relatively low-mass haloes (Fig. 7). This fact is of course well known at lower redshifts where a strong feedback is required to reproduce the faint-end of the galaxy luminosity function (e.g. Cole

et al. 2000), but is often ignored in reionization modelling, where a simple linear mass–luminosity relation is assumed.

(v) As also shown in the companion paper by Lacey et al. (2010a), the BAUGH05 model reproduces the observed $z \sim 6$–10 rest-frame 1500-Å luminosity functions well (Fig. 9), with bursts being a crucial ingredient in boosting the UV luminosities of galaxies to the observed levels. The good agreement between the predicted and observed UV luminosity functions gives credence to using the model for computing ϵ as well. In the model, ∼90 per cent of ionizing photons are produced by galaxies that are below the current *HST* detection limit at $z = 10$, with 50 per cent of ionizing photons produced by galaxies fainter than $m_{\rm AB} \sim 31$ in the *H*-band. The intrinsic faintness of the sources will make it very challenging to detect a significant fraction of the galaxies that caused reionization, even with *JWST*.

(vi) The shape of the rest-frame far-UV luminosity function in the BAUGH05 model resembles a Schechter function, but with significant departures due to bursts. Given that the $z \gtrsim 6$ data only probe the bright end of this LF, extrapolating a Schechter function fit to estimate the contribution from galaxies below the detection limit can be inaccurate (see the Appendix).

As in all models of reionization, a significant uncertainty is the fraction $f_{\rm esc}$ of ionizing photons produced by galaxies that can actually escape into the IGM. We have intentionally used a simple estimate for $f_{\rm esc}$, and our default value of 20 per cent is somewhat higher than found observationally in lower redshift observational studies (e.g. $f_{\rm esc} \sim 10$ per cent for LBGs at $z = 3$–4 Steidel et al. 2001). A high dust content, one of the consequences of using a top-heavy IMF, may decrease the escape fraction by as much as an order of magnitude (Benson et al. 2006). On the other hand, the fraction of the ionizing photons that can escape into the IGM during a burst could be significantly increased over the escape fraction during quiescent star formation, due to the galactic wind driven by the starburst. Detailed numerical models that include turbulent motions of gas in small galaxies find that $f_{\rm esc}$ can be as high as 0.5–1 *during* a burst (Fujita et al. 2003; Wise & Abel 2008; Wise & Cen 2009; Razoumov & Sommer-Larsen 2010). The enhancement of $f_{\rm esc}$ in bursts is likely to be more dramatic for smaller galaxies than for larger ones, hence the escape fraction is likely larger in small galaxies undergoing a burst. If this is the case, then small, bursting galaxies will dominate the Lyman-continuum emissivity even more. This strengthens our main conclusion that small, starbursting galaxies can reionize the Universe by $z \sim 10$. With this in mind, the value of $f_{\rm esc} = 0.2$ that we used throughout this paper may even be conservative.

As shown in the companion paper by Lacey et al. (2010a), the BAUGH05 GALFORM model reproduces the observed rest-frame 1500-Å luminosity function of high redshift galaxies well over the whole currently observed range $z = 3$–10. A crucial ingredient in this model is the boost in luminosity of galaxies as they undergo a minor or major merger, when the stellar initial mass function becomes top heavy. This top-heavy IMF in bursts was originally introduced in order to fit the counts of sub-millimetre galaxies at much lower $z \sim 2$, and is necessary also to reproduce the observed high metallicity of gas in $z \sim 0$ clusters of galaxies. A consequence is that bursts generate the majority of Lyman-continuum photons. The model predicts that starbursting galaxies with continuum UV magnitude $M_{1500,\rm AB} \sim -16$, in haloes of mass $\sim 10^9\,h^{-1}\,{\rm M}_\odot$, dominate the total emissivity at $z \sim 10$ (Fig. 5). The predicted properties of these galaxies have been analysed in more detail in Lacey et al. (2010a). Those authors show that these galaxies have stellar masses of $M_\star \sim 2 \times 10^5\,h^{-1}\,{\rm M}_\odot$, circular velocities $V_c \sim 40$ km s^{-1}, star formation rates $\dot{M}_\star \sim 0.06\,h^{-1}\,{\rm M}_\odot\,{\rm yr}^{-1}$, are gas dominated, $M_{\rm gas}/M_{\rm baryon} \sim 1$ and have gas and stellar metallicities of $\sim 4 \times 10^{-3}$ and $\sim 3 \times 10^{-3}$, respectively. Assuming that on average approximately two ionizing photons are required per hydrogen atom to reionize the Universe, a mean escape fraction of 20 per cent is sufficient to reionize the Universe by $z = 10$.

ACKNOWLEDGMENTS

We would like to thank the GALFORM team for allowing us to run their code, and for their constructive criticism. MR thanks John Helly, Violeta Gonzalez-Perez, Wong Tam and Carton Baugh for practical help and crucial discussions. During the work on this paper, MR was supported by a grant from Microsoft Research Cambridge.

REFERENCES

Bahcall J. N., Salpeter E. E., 1965, ApJ, 142, 1677
Barkana R., Loeb A., 2001, Phys. Rep., 349, 125
Baugh C. M., 2006, Rep. Prog. Phys., 69, 3101
Baugh C. M., Lacey C. G., Frenk C. S., Granato G. L., Silva L., Bressan A., Benson A. J., Cole S., 2005, MNRAS, 356, 1191
Becker G. D., Rauch M., Sargent W. L. W., 2007, ApJ, 662, 72
Benson A. J., Lacey C. G., Baugh C. M., Cole S., Frenk C. S., 2002a, MNRAS, 333, 156
Benson A. J., Frenk C. S., Lacey C. G., Baugh C. M., Cole S., 2002b, MNRAS, 333, 177
Benson A. J., Bower R. G., Frenk C. S., Lacey C. G., Baugh C. M., Cole S., 2003, ApJ, 599, 38
Benson A. J., Sugiyama N., Nusser A., Lacey C. G., 2006, MNRAS, 369, 1055
Bolton J. S., Haehnelt M. G., 2007, MNRAS, 382, 325
Bouwens R. J. et al., 2003, ApJ, 595, 589
Bouwens R. J., Illingworth G. D., Franx M., Ford H., 2007, ApJ, 670, 928
Bouwens R. J., Illingworth G. D., Franx M., Ford H., 2008, ApJ, 686, 230
Bouwens R. J. et al., 2009, preprint (arXiv:0912.4263)
Bouwens R. J. et al., 2010, ApJ, 709, 133
Bower R. G., Benson A. J., Malbon R., Helly J. C., Frenk C. S., Baugh C. M., Cole S., Lacey C. G., 2006, MNRAS, 370, 645
Boylan-Kolchin M., Springel V., White S. D. M., Jenkins A., Lemson G., 2009, MNRAS, 398, 1150
Bressan A., Granato G. L., Silva L., 1998, A&A, 332, 135
Bunker A., Stanway E., Ellis R., Lacy M., McMahon R., Eyles L., Stark D., Chiu K., 2009a, preprint (arXiv:0909.1565)
Bunker A. et al., 2009b, preprint (arXiv:0909.2255)
Choudhury T. R., Ferrara A., 2007, MNRAS, 380, L6
Ciardi B., Ferrara A., 2005, Space Sci. Rev., 116, 625
Ciardi B., Bianchi S., Ferrara A., 2002, MNRAS, 331, 463
Ciardi B., Stoehr F., White S. D. M., 2003, MNRAS, 343, 1101
Ciardi B., Scannapieco E., Stoehr F., Ferrara A., Iliev I. T., Shapiro P. R., 2006, MNRAS, 366, 689
Clarke C., Oey M. S., 2002, MNRAS, 337, 1299
Cole S., Lacey C. G., Baugh C. M., Frenk C. S., 2000, MNRAS, 319, 168
Cole S. et al., 2001, MNRAS, 326, 255
Crain R. A. et al., 2009, MNRAS, 399, 1773
Croton D. J. et al., 2006, MNRAS, 365, 11
Dekel A., Silk J., 1986, ApJ, 303, 39
Efstathiou G., 1992, MNRAS, 256, 43P
Fan X. et al., 2003, AJ, 125, 1649
Fujita A., Martin C. L., Mac Low M., Abel T., 2003, ApJ, 599, 50
Fukugita M., Hogan C. J., Peebles P. J. E., 1998, ApJ, 503, 518
Furlanetto S. R., Zaldarriaga M., Hernquist L., 2004, ApJ, 613, 1
Giallongo E., Cristiani S., D'Odorico S., Fontana A., 2002, ApJ, 568, L9
Gnedin N. Y., 2000a, ApJ, 535, 530
Gnedin N. Y., 2000b, ApJ, 542, 535

Gnedin N. Y., Ostriker J. P., 1997, ApJ, 486, 581
González J. E., Lacey C. G., Baugh C. M., Frenk C. S., Benson A. J., 2009, MNRAS, 397, 1254
Gonzalez-Perez V., Baugh C. M., Lacey C. G., Almeida C., 2009, MNRAS, 398, 497
Gunn J. E., Peterson B. A., 1965, ApJ, 142, 1633
Hernquist L., Mihos J. C., 1995, ApJ, 448, 41
Hoeft M., Yepes G., Gottlöber S., Springel V., 2006, MNRAS, 371, 401
Iliev I. T., Mellema G., Pen U., Merz H., Shapiro P. R., Alvarez M. A., 2006, MNRAS, 369, 1625
Kennicutt R. C., 1983, ApJ, 272, 54
Komatsu E. et al., 2010, preprint (arXiv:1001.4538)
Lacey C., Cole S., 1993, MNRAS, 262, 627
Lacey C. G., Baugh C. M., Frenk C. S., Silva L., Granato G. L., Bressan A., 2008, MNRAS, 385, 1155
Lacey C. G., Baugh C. M., Frenk C. S., Benson A. J., 2010a, preprint (arXiv:1004.3545)
Lacey C. G., Baugh C. M., Frenk C. S., Benson A. J., Orsi A., Silva L., Granato G. L., Bressan A., 2010b, MNRAS, 405, 2
Larson R. B., 1998, MNRAS, 301, 569
Le Delliou M., Lacey C. G., Baugh C. M., Morris S. L., 2006, MNRAS, 365, 712
Loeb A., 2006, preprint (arXiv:astro-ph/0603360)
Loeb A., 2009, J. Cosmol. Astropart. Phys., 3, 22
Madau P., Meiksin A., Rees M. J., 1997, ApJ, 475, 429
Madau P., Haardt F., Rees M. J., 1999, ApJ, 514, 648
McQuinn M., Lidz A., Zahn O., Dutta S., Hernquist L., Zaldarriaga M., 2007, MNRAS, 377, 1043
Nagashima M., Lacey C. G., Okamoto T., Baugh C. M., Frenk C. S., Cole S., 2005a, MNRAS, 363, L31
Nagashima M., Lacey C. G., Baugh C. M., Frenk C. S., Cole S., 2005b, MNRAS, 358, 1247
Oesch P. A. et al., 2009, ApJ, 709, 160
Oh S. P., 2001, ApJ, 553, 499
Okamoto T., Gao L., Theuns T., 2008, MNRAS, 390, 920
Orsi A., Lacey C. G., Baugh C. M., Infante L., 2008, MNRAS, 391, 1589
Parkinson H., Cole S., Helly J., 2008, MNRAS, 383, 557
Patel M., Warren S. J., Mortlock D. J., Fynbo J. P. U., 2010, A&A, 512, 3
Pawlik A. H., Schaye J., van Scherpenzeel E., 2009, MNRAS, 394, 1812
Press W. H., Schechter P., 1974, ApJ, 187, 425
Razoumov A. O., Sommer-Larsen J., 2010, ApJ, 710, 1239
Salvaterra R., Ferrara A., Dayal P., 2010, preprint (arXiv:1003.3873)
Schaye J., Theuns T., Rauch M., Efstathiou G., Sargent W. L. W., 2000, MNRAS, 318, 817
Schmidt M., 1965, ApJ, 141, 1295
Shapiro P. R., Iliev I. T., Raga A. C., 2004, MNRAS, 348, 753
Shapley A. E., Steidel C. C., Pettini M., Adelberger K. L., Erb D. K., 2006, ApJ, 651, 688
Shaver P. A., Windhorst R. A., Madau P., de Bruyn A. G., 1999, A&A, 345, 380
Sokasian A., Abel T., Hernquist L., Springel V., 2003, MNRAS, 344, 607
Springel V. et al., 2005, Nat, 435, 629
Steidel C. C., Giavalisco M., Pettini M., Dickinson M., Adelberger K. L., 1996, ApJ, 462, L17
Steidel C. C., Pettini M., Adelberger K. L., 2001, ApJ, 546, 665
Theuns T., Schaye J., Zaroubi S., Kim T., Tzanavaris P., Carswell B., 2002, ApJ, 567, L103
Totani T., Kawai N., Kosugi G., Aoki K., Yamada T., Iye M., Ohta K., Hattori T., 2006, PASJ, 58, 485
Tozzi P., Madau P., Meiksin A., Rees M. J., 2000, ApJ, 528, 597
Trac H., Cen R., 2007, ApJ, 671, 1
Trac H., Gnedin N. Y., 2009, preprint (arXiv:0906.4348)
Volonteri M., Gnedin N. Y., 2009, ApJ, 703, 2113
White S. D. M., Frenk C. S., 1991, ApJ, 379, 52
Wise J. H., Abel T., 2008, ApJ, 684, 1
Wise J. H., Cen R., 2009, ApJ, 693, 984
Wyithe J. S. B., Cen R., 2007, ApJ, 659, 890
Zafar T., Watson D. J., Malesani D., Vreeswijk P. M., Fynbo J. P. U., Hjorth J., Levan A. J., Michałowski M. J., 2010, A&A, 515, 94

APPENDIX A: INFERRING IONIZING EMISSIVITY FROM SCHECHTER FITS TO THE LF

In observational studies, the contribution of galaxies below the detection threshold to the total ionizing emissivity is usually estimated by fitting the observed LF with a Schechter function (e.g. Bouwens et al. 2007; Bunker et al. 2009b). At first glance, the far-UV LFs predicted by the BAUGH05 model and shown in this paper are indeed reasonably well represented by Schechter functions, as they have a power-law shape at low luminosity, $\propto L^{\alpha}$, and an exponential drop-off at the high-luminosity end, $\propto \exp(-L/L_{\star})$. However, the LFs predicted by GALFORM are *not* in detail described well by Schechter functions. In particular, in the BAUGH05 model, starbursts introduce a feature (a 'bump') at $\sim$2 magnitudes below $L_{\star}$ at high redshifts [see Lacey et al. (2010a) for more details]. Due to this departure from the Schechter shape, the result of fitting a Schechter function to a GALFORM LF is strongly dependent on the luminosity range over which the fit is done (Fig. A1). Assuming that BAUGH05 is the 'correct' model of the high-z galaxy population, the observational detection limits will then strongly affect the predicted total ionizing emissivity, which relies on extrapolating the contribution of the currently unobserved low-luminosity galaxies based on the faint-end slope α of the Schechter fit. We want to investigate how much such extrapolations are likely to be in error.

The estimated LC emissivity depends on more than just the LF shape, with the choice of IMF and dust extinction being crucial yet only weakly constrained by current observations. To focus only on

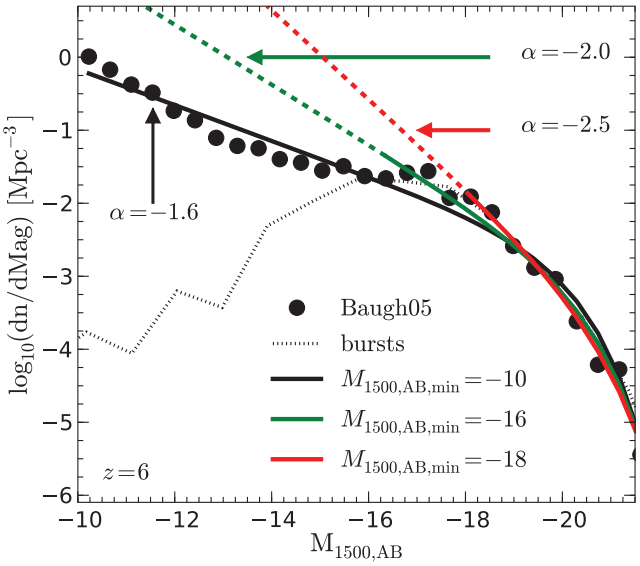

Figure A1. Schechter function fits (coloured lines) to the far-UV LF in the BAUGH05 model (heavy dots) at $z = 6$ over different absolute magnitude ranges, extrapolated to fainter luminosities (dashed lines). Starbursts (dotted line) introduce a deviation in the shape of the LF from a Schechter function. Due to this feature, varying the minimum absolute magnitude employed in the Schechter fit results in very different estimates of the faint-end slope parameter, α^* (black, green and red lines correspond to minimum values of $M_{1500,\mathrm{AB}}$ of -10, -16 and -18, respectively). Extrapolation of the fits to fainter values can then lead to inaccurate estimates of luminosity density (see Fig. A2), which in turn results in wrongly estimated LC emissivities.

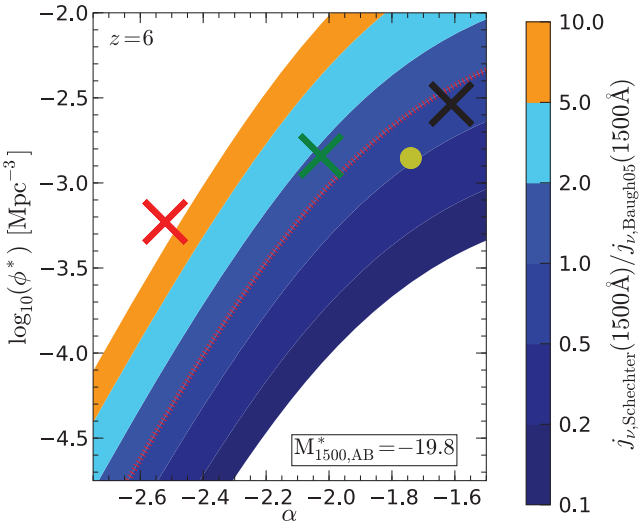

Figure A2. Comparison of the 1500-Å luminosity densities, j_ν, obtained by integrating the Schechter function fits to the BAUGH05 model LF at $z = 6$, with the values obtained from integrating over the true model LF at the same redshift. The colour shading indicates the ratio of the luminosity density from the Schechter fit to the actual value in the model. In the Schechter fits, $M^*_{1500,AB}$ is held fixed at its best-fitting value for the full luminosity range (black line in Fig. A1), while α and ϕ^* are the best-fitting values for each choice of the minimum $M_{1500,AB}$. Values of (α, ϕ^*) along the *dotted red line* reproduce the actual luminosity density of the BAUGH05 model. Crosses mark the parameters of the three fits shown in Fig. A1, plotted in the same colours. When the whole luminosity range is used for the fit (black cross), the model luminosity density is reasonably well reproduced by the integral over the Schechter function fit. On the other hand, fits performed on a more limited luminosity range, as in Fig. A1, lead to significant errors in the luminosity density estimate. The yellow dot shows the results obtained with the best-fitting parameters from Bouwens et al. (2007) at this redshift.

the uncertainty from the assumed LF shape, in Fig. A2 we show the dependence of the 1500-Å luminosity density, j_ν, on the Schechter fit parameters. All values of j_ν were obtained by integrating the LFs over the magnitude range $-22 < M_{1500,AB} < -10$. In this figure, we vary only the normalization, $\phi^\star$, and the faint-end power-law slope, α, and keep the characteristic absolute magnitude, $M^\star_{1500,AB}$, fixed, because the fits shown in Fig. A1 clearly have very similar $M^\star_{1500,AB}$ values.

With this procedure, a Schechter fit over the whole luminosity range (down to $M_{1500,AB} = -10$, black line in Fig. A1) of the BAUGH05 LF provides a good estimate of the real luminosity density in the model (black cross in Fig. A2; the luminosity density from the fit is ∼20 per cent lower than the original model). If instead the Schechter function is fit only to the brighter part of the LF (green and red crosses, corresponding to $M_{1500,AB,min}$ of -16 and -18, respectively), the faint-end slope of the model is strongly overestimated. As a result, the luminosity density is also overestimated in these cases, by factors of ∼2 and 30 for $M_{1500,AB,min} = -16$ and -18, respectively. We note that the BAUGH05 model predicts a total 1500-Å luminosity density at $z = 6$ a few times larger than estimates based on integrating the observed LF only over the currently observed luminosity range (e.g. Bouwens et al. 2007), but this difference shrinks if the observed Schechter fits are extrapolated to lower luminosities (e.g. the yellow circle in Fig. A2 shows the Schechter fit found by Bouwens et al., which implies a luminosity density only two times lower than found in the model). Some authors have concluded from integrating over the observed far-UV LFs at $z \gtrsim 7$ that galaxies alone do not emit enough ionizing photons to keep the Universe ionized at these redshifts (see e.g. Bunker et al. 2009b), but such conclusions seem premature, given that they do not allow for galaxies fainter than the current detection threshold or dust extinction or a different IMF slope.

This exercise aims to point out the danger of using Schechter function fits to the observational data to estimate ionizing emissivity produced by high-z galaxies. The deviations of the LF from the Schechter shape only add more uncertainty to the procedure which already hinges on a number of unknowns, e.g. the choice of the IMF and the dust extinction. This becomes even more important at higher redshifts, where the LF is even more poorly constrained by current observational data.

This paper has been typeset from a TEX/LATEX file prepared by the author.